



This is a repository copy of *A dynamic conductance model of fluorescent lamp for electronic ballast design simulation*.

White Rose Research Online URL for this paper:

<http://eprints.whiterose.ac.uk/783/>

Article:

Loo, K.H., Stone, D.A., Tozer, R.C. et al. (1 more author) (2005) A dynamic conductance model of fluorescent lamp for electronic ballast design simulation. *IEEE Transactions on Power Electronics*, 20 (5). pp. 1178-1185. ISSN 0885-8993

<https://doi.org/10.1109/tpel.2005.854057>

Reuse

Unless indicated otherwise, fulltext items are protected by copyright with all rights reserved. The copyright exception in section 29 of the Copyright, Designs and Patents Act 1988 allows the making of a single copy solely for the purpose of non-commercial research or private study within the limits of fair dealing. The publisher or other rights-holder may allow further reproduction and re-use of this version - refer to the White Rose Research Online record for this item. Where records identify the publisher as the copyright holder, users can verify any specific terms of use on the publisher's website.

Takedown

If you consider content in White Rose Research Online to be in breach of UK law, please notify us by emailing eprints@whiterose.ac.uk including the URL of the record and the reason for the withdrawal request.

A Dynamic Conductance Model of Fluorescent Lamp for Electronic Ballast Design Simulation

Ka Hong Loo, *Member, IEEE*, Dave A. Stone, Richard C. Tozer, *Senior Member, IEEE*, and Robin Devonshire

Abstract—A Spice-compatible dynamic conductance model of a fluorescent lamp for use in electronic ballast simulation is presented. The time-dependent conductance of the fluorescent lamp is derived from a plasma ionization balance equation that uses simplified descriptions of the physical processes within the lamp as its basis. The model has been designed to enable user-defined lamp radius, length, buffer gas pressure and cold-spot temperature as input parameters thus representing a valuable tool for ballast simulations. Simulation results are compared to experimental measurements and satisfactory agreement is achieved.

Index Terms—Discharge model, electronic ballast, fluorescent lamp, fluorescent lamp model, gas discharge lamp, low-pressure discharge lamp.

I. INTRODUCTION

LIGHTING currently consumes approximately 10–15% of the global energy requirement [1]. Given the increasing concerns about energy saving, an urgent need to improve the efficiency of lighting systems proves to be of significant importance. For general lighting, fluorescent lamps are known for decades to be an efficient light source mainly used for home and office lighting. Today approximately 1.2 billion units of these lamps are manufactured worldwide each year [1]. A fluorescent lamp is essentially a low-pressure mercury-argon discharge held in a cylindrical tube with phosphor coating that converts the ultraviolet radiation produced into visible light. Its relative merits compared to incandescent lamps include energy saving and longer life.

During recent years, fluorescent lamps operating at high frequency have emerged as energy-efficient alternatives to replace the conventional 50/60-Hz systems and also the incandescent lamps in the form of compact fluorescent lamps (CFL). Advantages of driving fluorescent lamps at high frequency include increased light output, elimination of flicker and audible noise, lower ballast power consumption and extended lamp life. To accommodate these changes, the conventional 50/60-Hz electromagnetic ballasts are also gradually replaced with the more energy-efficient high-frequency electronic ballasts. These new

ballasts also offer additional features such as compactness in size and light in weight, dimming capability and power factor correction.

Computer simulation using the widely used circuit simulators such as Spice, Saber, and Simulink has become an indispensable tool in the industrial development of electronic ballast. These simulators, however, do not incorporate lamp models into their standard libraries and the users are therefore faced with the challenge to devise these models separately. Many previously reported fluorescent lamp models [2]–[4] have approximated the lamp as a power-dependent linear resistor or simply a resistor with a cubic voltage-current characteristic. In general such models are not physically self-consistent and require empirical fittings on data obtained from lamp measurements. Their range of applicability is also limited to the conditions under which such data can be measured.

A dynamic conductance model of fluorescent lamp derived from the time-dependent plasma ionization balance equation is presented here. The model does not require any external data from lamp measurements but relies only on the intrinsic plasma data that can be derived from separate calculations. Once determined, these data needs no further adjustment to account for parameter changes arising from the changes in operating conditions. In the following section, the theory of the proposed model is given. Lamp data are measured for both 50 Hz and high-frequency operations and compared to simulation results in Section III. From these, a satisfactory agreement is demonstrated.

II. LAMP MODEL

A. Francis Equation

A general differential equation is derived by Francis [5] to describe the dynamic characteristics of any discharge tube. The formulation employs three lamp variables: average electron density, lamp voltage and lamp current, and is based on the following three postulates.

- 1) The rate of electron production in the discharge column is proportional to the current and voltage.
- 2) The rate of loss of electrons is proportional to the electron density.
- 3) The instantaneous resistance of the discharge (v_L/i_L) is inversely proportional to the electron density.

From Postulate 1 and 2, we have the following differential equation, where α and β are constants

$$\frac{dn_e}{dt} = \alpha v_L i_L - \beta n_e. \quad (1)$$

Manuscript received August 20, 2003; revised December 16, 2004. Recommended by Associate Editor R.-L. Lin.

K. H. Loo is with the Department of Electronic and Electrical Engineering, University of Sheffield, Sheffield S1 3JD, U.K. and also with the Department of Electrical and Electronic Engineering, Ehime University, Ehime 790-8577, Japan (e-mail: k.h.loo@ieee.org).

D. A. Stone and R. C. Tozer are with the Department of Electronic and Electrical Engineering, University of Sheffield, Sheffield S1 3JD, U.K.

R. Devonshire is with the High Temperature Science Laboratories, Department of Chemistry, University of Sheffield, Sheffield S3 7HF, U.K.

Digital Object Identifier 10.1109/TPEL.2005.854057

From Postulate 3, we have the following equation, where F is a constant

$$\frac{v_L}{i_L} = \frac{F}{n_e}. \quad (2)$$

Substitution of (2) into (1) gives

$$\frac{dn_e}{dt} = \left(\frac{\alpha}{F} v_L^2 - \beta \right) n_e. \quad (3)$$

Using Postulate 3 and the relationship $\sigma = i_L/v_L$, where σ is the discharge conductance, one can rearrange (3) in a form that is more useful for circuit analysis.

This gives

$$\frac{d\sigma}{dt} = \left(\frac{\alpha}{F} v_L^2 - \beta \right) \sigma. \quad (4)$$

It was suggested by Francis that the constants α , β , and F were not arbitrary but were functions of the tube dimensions and the gas filling. In fact the equation of the form given by (3) is a plasma ionization balance equation and in the following section the parameters determining the balance are derived more systematically than in the simplified approach employed by Francis.

B. Plasma Ionization Balance Equation

The “positive column” region of a discharge occupies nearly the entire axial length of the discharge and dissipates typically in excess of 85% of the electrical power input to the lamp. It is assumed in this model that the cathode and anode drops are small compared to the voltage drop across the positive column. Due to its quasi-neutrality nature, the term “plasma” is usually used to describe the positive column. In a steady-state plasma driven by direct current, the number of electrons produced in a volume is balanced by the number of electrons that diffuse to the wall and subsequently recombine [6]

$$\nu_i = D_a \nabla^2 \left(\frac{n_e}{n_{e0}} \right) \Leftrightarrow \nu_i - D_a \nabla^2 \left(\frac{n_e}{n_{e0}} \right) = 0 \quad (5)$$

where ν_i [s^{-1}] is the ionization rate, D_a [$m^2 s^{-1}$] is the ambipolar diffusion coefficient, n_e [m^{-3}] is the electron density and n_{e0} [m^{-3}] is the electron density at the discharge axis. D_a can be expanded and rewritten in terms of the electron temperature T_e [K] and the mercury ion mobility μ_{ion} [$m^2 V^{-1} s^{-1}$] [6]

$$D_a = \frac{k T_e \mu_{ion}}{e}. \quad (6)$$

For an argon-filled lamp, μ_{ion} can be approximated by (7), where T_{gas} [$^\circ C$] is the gas temperature and P_{argon} [Torr] is the argon pressure [7]

$$\mu_{ion} = 8.11 \times 10^{-3} \frac{(273 + T_{gas})^{1/2}}{P_{argon}}. \quad (7)$$

Applying the Schottky’s diffusion theory [8], which states that in low-pressure discharges the radial profile of electron density is described by the Bessel function J_0 , the following simplification can be made

$$\begin{aligned} n_e &= n_{e0} J_0 \left(\frac{2.4r}{R} \right) \\ &\Rightarrow \nabla^2 \left(\frac{n_e}{n_{e0}} \right) = \left(\frac{2.4}{R} \right)^2 = \frac{5.76}{R^2} \end{aligned} \quad (8)$$

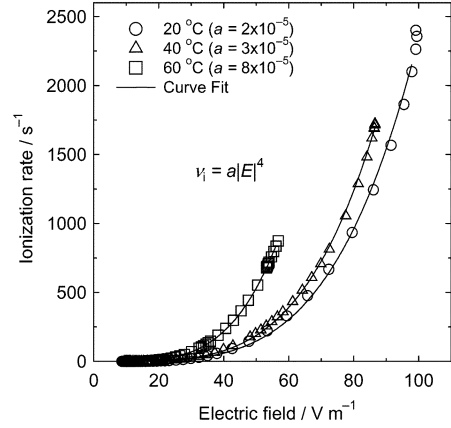


Fig. 1. Ionization rates calculated as a function of the electric field at various cold-spot temperatures (lamp configuration— $R = 0.018$ m, $L = 1.2$ m, $P_{argon} = 3$ Torr).

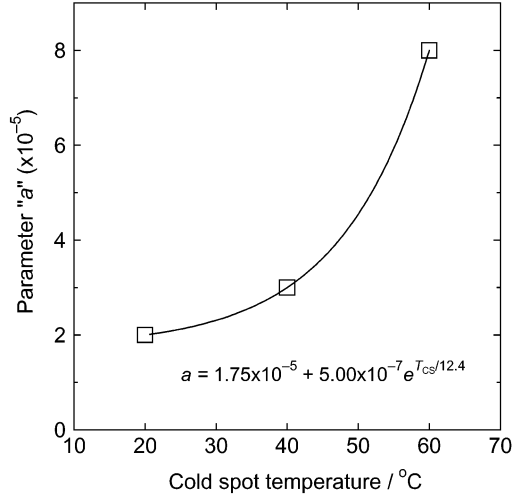


Fig. 2. Parameter “a” fitted using an exponential growth function of the cold-spot temperature.

where R [m] is the lamp radius. Under transient condition, e.g., alternating current, the ionization balance equation is modified to include an additional time-dependent term [6]

$$\nu_i = D_a \frac{5.76}{R^2} + \frac{1}{n_e} \frac{dn_e}{dt}. \quad (9)$$

Rearranging (9) gives

$$\frac{dn_e}{dt} = \left(\nu_i - D_a \frac{5.76}{R^2} \right) n_e. \quad (10)$$

Equation (10) is the plasma ionization balance equation, which states that the rate of change of electron density under transient conditions is determined by the balance between the production rate of electrons by ionization and the loss rate of electrons by diffusion to the wall. Other recombination mechanisms such as impact-radiative and molecular dissociative recombination are assumed to play a negligible role in the overall recombination process. By comparing the corresponding terms in (3) and (10) we can write down the following relationships:

$$\frac{\alpha}{F} v_L^2 = \nu_i \Rightarrow \psi_{ion} = f(v_L) \quad (11)$$

$$\beta = D_a \frac{5.76}{R^2} \Rightarrow \psi_{dif} = f(T_e, T_{gas}, P_{argon}, R). \quad (12)$$

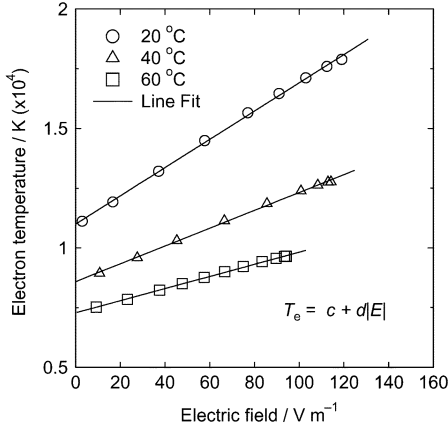


Fig. 3. Electron temperature calculated as a function of the electric field at various cold-spot temperatures (lamp configuration— $R = 0.018$ m, $L = 1.2$ m, $P_{\text{argon}} = 3$ Torr).

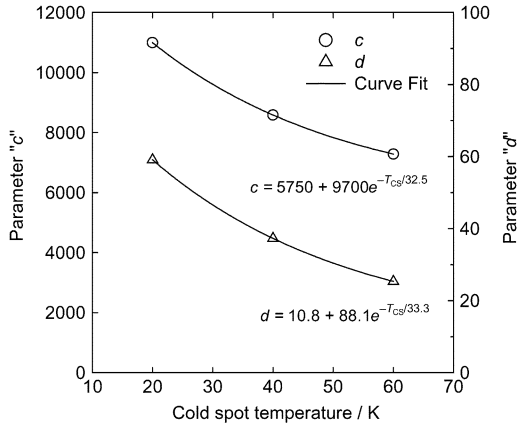


Fig. 4. Parameter "c" and "d" fitted using exponential decay functions of the cold-spot temperature.

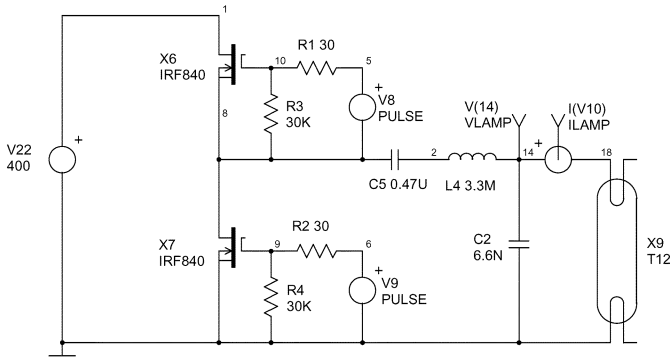


Fig. 5. Schematic diagram of the dimmable high-frequency electronic ballast used to validate the proposed model in Spice.

Since the electrons that produce ionization gain their energy from the electric field, whose value is derived from the lamp voltage, the relationship suggested by (11) appears to be physically sensible. Nevertheless, by intuition the ionization rate cannot be a function of the lamp voltage alone because it must also depend on the number of mercury atoms available for ionization. The given equation is therefore only applicable when the lamp is operating at a given mercury vapor pressure or cold-spot temperature T_{CS} [°C] (temperature of the glass

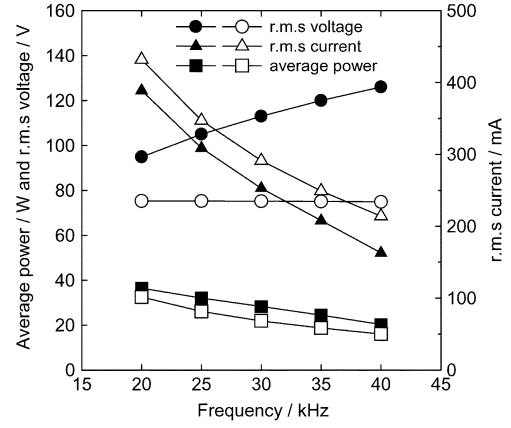


Fig. 6. Measured and simulated r.m.s voltages, r.m.s currents and average lamp powers at various frequencies: (a) 40-W and (b) 20-W rated lamps. Solid and hollow marks indicate the measured and simulated values, respectively.

wall that controls the operating mercury vapor pressure). In order to generalize the model, the ionization rate must also be made as a function of the cold-spot temperature T_{CS} so that $\psi_{\text{ion}} = f(T_{\text{CS}}, v_L)$.

C. Functional Fits for Ionization and Diffusion Rates

In this section, functional fits are obtained for the ionization and diffusion rates by finding simplified relationships between these rates and their controlling parameters. As these relationships are not easily found from experimental measurements, they are calculated theoretically using a collisional-radiative plasma model based on coupled rate equations that describe microscopic electron and heavy particle collisions and radiative processes. The detailed description of the plasma model used for these calculations is given elsewhere [9], [10]. Data extracted from this plasma model are described henceforth in this paper as "calculated" data.

Fig. 1 shows the calculated ionization rates as a function of the electric field at the cold-spot temperatures of 20, 40, and 60 °C. The power law function $\nu_i = aE^b$ is shown to be a satisfactory fit to the calculated data. Since the electric field in the plasma is axially uniform [11], and since electrode drops are being neglected, it can be obtained directly from the lamp voltage using the relationship $E = v_L/L$, where L is the axial length of the lamp. During the fitting procedure, the exponent of

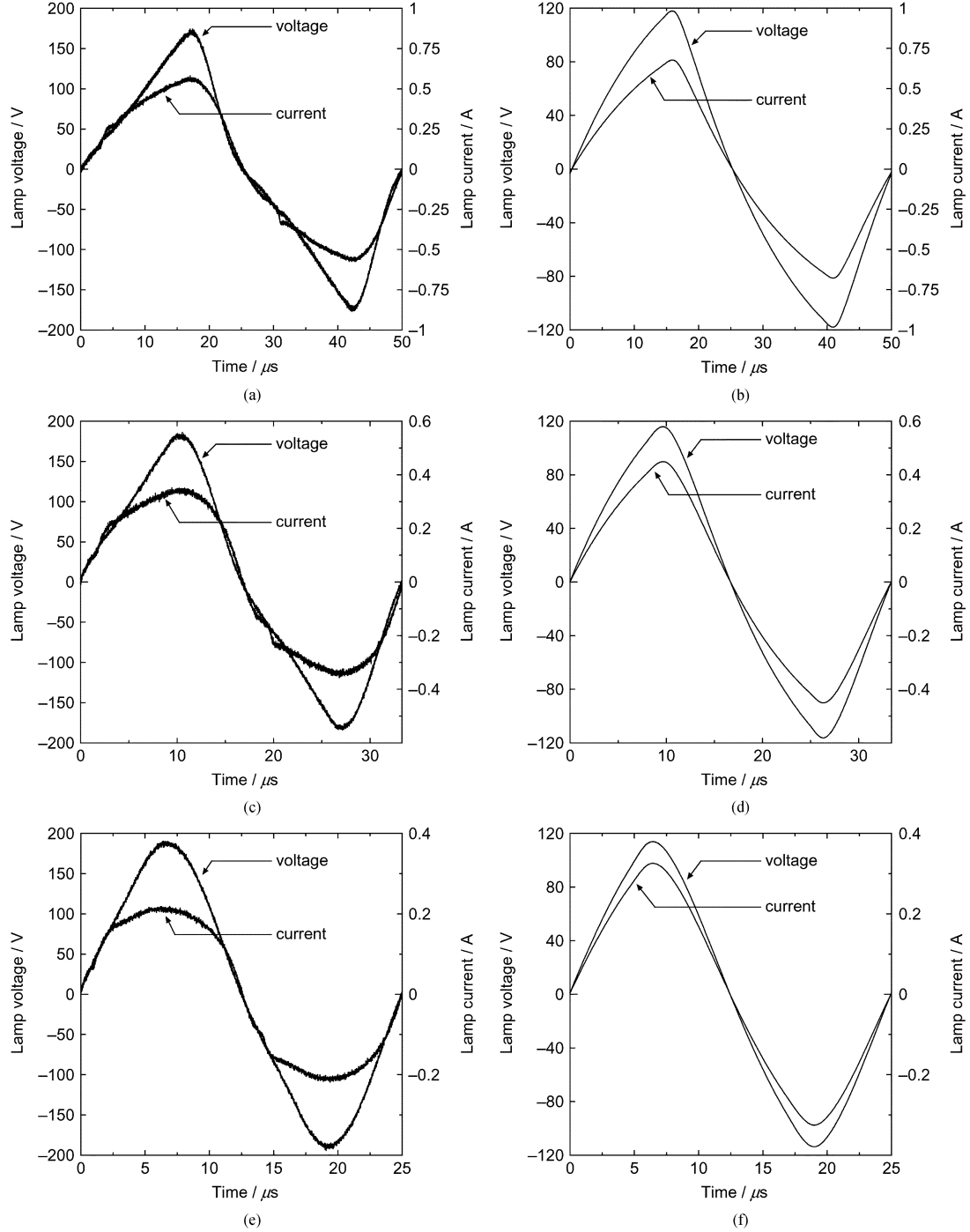


Fig. 7. Measured and simulated lamp voltage and current waveforms at various frequencies: (a) 20 kHz (measured), (b) 20 kHz (simulated), (c) 30 kHz (measured), (d) 30 kHz (simulated), (e) 40 kHz (measured), and (f) 40 kHz (simulated).

E is kept constant at $b = 4$ while the parameter “ a ” is made to be a function of the cold-spot temperature T_{CS} . A satisfactory fit for the parameter “ a ” is given by the exponential function shown in Fig. 2. Hence, we have

$$\psi_{ion} = a|v_L/L|^4 \quad (13)$$

$$a = 1.75 \times 10^{-5} + 5.00 \times 10^{-7} \exp(T_{CS}/12.4). \quad (14)$$

From (6), (7), and (12)

$$\psi_{dif} = 4.03 \times 10^{-6} \frac{T_e (273 + T_{gas})^{1/2}}{P_{argon} R^2}. \quad (15)$$

P_{argon} , R , and T_{gas} are taken as user-defined model parameters. The electron temperature T_e is directly proportional to the average electron energy ($=3kT_e/2$) so it is expected to be a function of the electric field E and hence the lamp voltage v_L . The relationship between T_e and E is depicted in Fig. 3. The functional fits for T_e , the parameters “ c ” and “ d ” are given by

$$T_e = c + d|v_L/L| \quad (16)$$

$$c = 5750 + 9700 \exp(-T_{CS}/32.5) \quad (17)$$

$$d = 10.8 + 88.1 \exp(-T_{CS}/33.3). \quad (18)$$

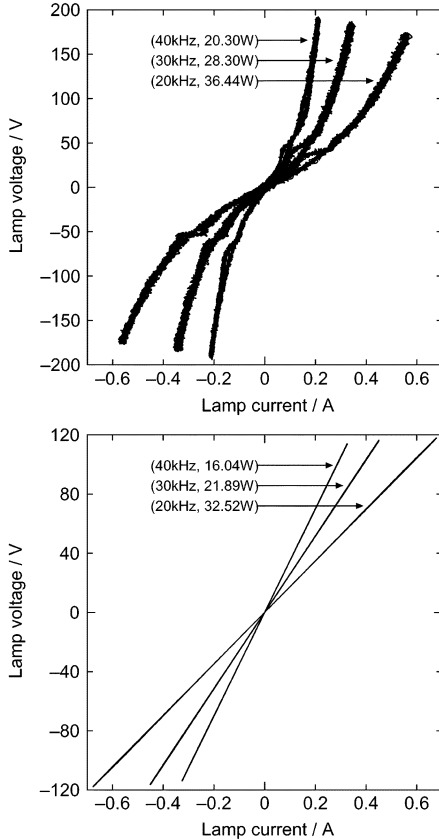


Fig. 8. Lamp voltage-current characteristics at various frequencies and average powers: (a) measured and (b) simulated.

Finally, by treating the lamp as a circuit element with conductance σ , (10) is rewritten as (19) in terms of the lamp conductance in a similar way to (4). The time-dependent lamp conductance is then obtained by numerically integrating (20), where σ_0 is the initial lamp conductance

$$\frac{d\sigma}{dt} = (\psi_{ion} - \psi_{dif}) \sigma \quad (19)$$

$$\sigma(t) = \sigma_0 \exp \int_0^t (\psi_{ion} - \psi_{dif}) dt. \quad (20)$$

III. MODEL VERIFICATIONS

The fluorescent lamp model is implemented in a Spice simulator according to the following procedure. The model is first set up to prompt the user for model input parameters including the lamp radius, length, argon pressure, cold-spot temperature and gas temperature. Using these parameters, the model then computes the parameters “a,” “c,” and “d” using (14), (17), and (18), respectively, which are further inserted into (13) and (15) to calculate ψ_{ion} and ψ_{dif} . All these calculations are performed using the arbitrary voltage source (B-element) function provided by Spice. The voltage difference between ψ_{ion} and ψ_{dif} is passed into an integrator and an exponential math function blocks to perform the calculations required by (20) to produce the new lamp conductance σ . Finally, the new lamp voltage v_L is determined from the lamp current i_L by using the Ohm’s law $i_L = \sigma v_L$ Fig. 4.

In this section, the proposed model is used to simulate two 38-mm diameter tubular fluorescent lamps with power ratings

of 20 W (Toshiba FL20S-W, $L = 0.6$ m) and 40 W (Toshiba FLR40S-D/M/36, $L = 1.2$ m), respectively. Both these lamps are by default filled with 3 Torr of argon and the typical gas temperature is between 50 °C ($I_{rms} = 100$ mA) and 70 °C ($I_{rms} = 600$ mA) [12]. The commercial 26-mm diameter lamps that are filled with krypton(75%)-argon(25%) are not used for verification because they do not correspond to the argon-filled lamps that we attempt to model. A dimmable ballast of the topology shown in Fig. 5 has been constructed to measure the lamp voltage and current waveforms for the frequency range 20–40 kHz. The corresponding r.m.s. voltages and currents are calculated from the measured waveforms and compared to simulation results. To show the applicability of the model at low frequency, voltage and current waveforms are also measured on the 40-W lamp operated at 50 Hz using inductive ballast.

Fig. 6(a) shows the variations of the r.m.s voltage, r.m.s current and average lamp power of the 40-W lamp with ballast frequency. Fig. 6(b) shows a similar graph but on the 20-W lamp. Measurements show that as the frequency is increased, there is a corresponding decrease of the r.m.s current delivered to the lamp due to the increased impedance of the series ballast inductance. This is accompanied by a slight increase in the r.m.s voltage as suggested by the negative resistance behavior of the lamp. The combined trend of voltage and current behavior therefore gives rise to an overall decrease of the average lamp power. In general, the r.m.s current and average power values predicted by the model follow quite closely the measured ones that both sets of values in fact vary approximately in parallel to one another. Since the positive column typically consumes about 85% of the total input power, where the rest is consumed in the electrode region that is excluded from the model, normalizing the average power curve by 0.85 brings the predicted curve closer to the measured one.

While the negative resistance behavior of discharge lamp suggests that a decreasing lamp voltage always accompanies an increasing lamp current due to the ionization contribution from the excited atomic states, the model’s prediction suggests that the lamp voltage is independent of the lamp current. Such contradiction arises as a feature of the oversimplified approach taken in formulating the Francis equation. This can be explained by solving the equation for the steady-state case $dn_e/dt = 0$ which corresponds to the condition under direct current and high frequency discharges.

From (3)

$$\frac{\alpha}{F} v_L^2 - \beta = 0 \Rightarrow v_L = \sqrt{\frac{\beta F}{\alpha}}. \quad (21)$$

If the lamp geometry, argon pressure and cold-spot temperature are kept constant, (21) suggests that the parameters α , β , F and hence the lamp voltage v_L are constant and independent of the drive conditions. Nevertheless, obtaining a similar expression of v_L based on the ionization balance gives some insights into the possibilities of resolving this disagreement. From (10), (13), (15), and (16)

$$\begin{aligned} \psi_{ion} &= \psi_{dif} \Rightarrow \frac{|v_L/L|^4}{c + d|v_L/L|} \\ &= \frac{4.0288 \times 10^{-6}}{a} \frac{(273 + T_{gas})^{1/2}}{P_{argon} R^2}. \end{aligned} \quad (22)$$

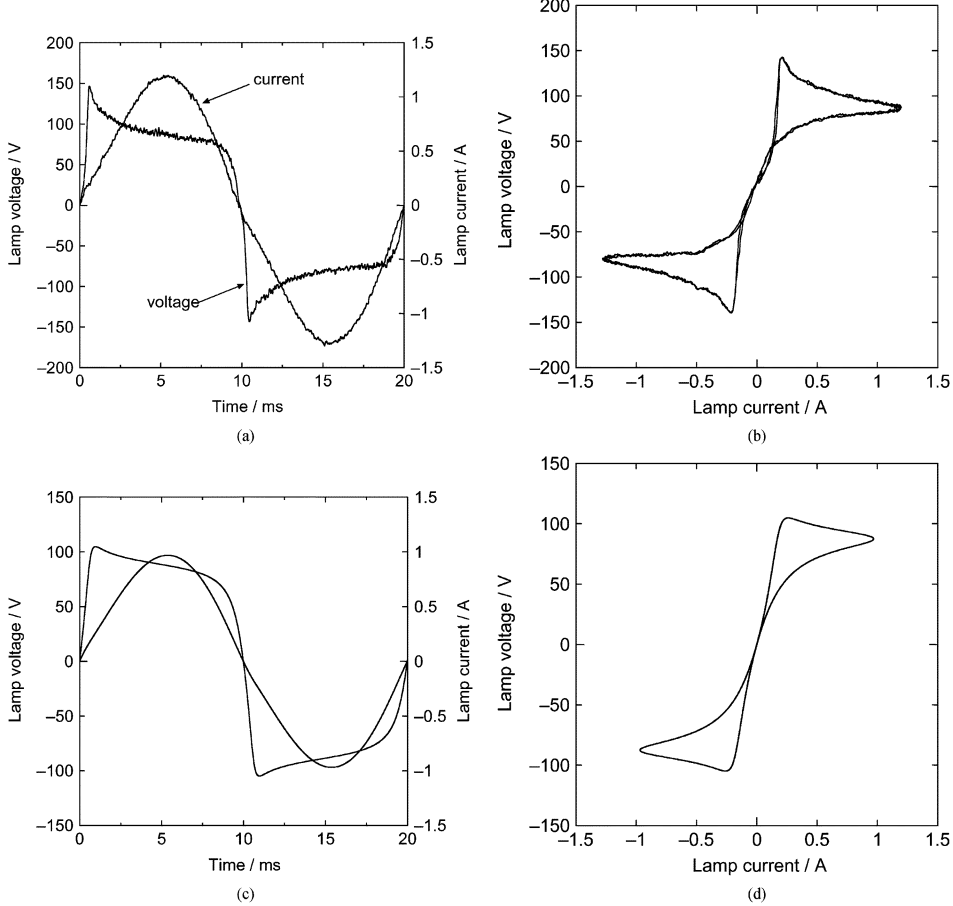


Fig. 9. Lamp voltage and current waveforms at 50 Hz: (a) measured and (c) simulated. Lamp voltage-current characteristics at 50 Hz: (b) measured and (d) simulated.

At first glance, T_{gas} appears to be the only candidate that will make v_L responsive to the drive conditions. This choice appears to be reasonable in practice as changes in the lamp current i_L would alter the heating effect it has on the plasma. If T_{gas} is made to increase with i_L while other parameters are kept constant, this would imply that the diffusion rate ψ_{dif} increases and a higher v_L is required to maintain the discharge, which gives rise to a positive resistance behavior. Now since $P_{\text{argon}} \propto T_{\text{gas}}$ from the ideal gas law, there must be a corresponding increase in P_{argon} as T_{gas} increases, and because ψ_{dif} decreases more rapidly with P_{argon} than it increases with T_{gas} , an overall decrease of ψ_{dif} and the maintaining voltage v_L is expected as i_L increases, which correctly predicts the negative resistance behavior. Therefore, in order to improve the model further, both T_{gas} and P_{argon} need to be functions of i_L .

Fig. 7(a)–(f) show the measured and simulated lamp voltage and current waveforms of the 40-W lamp operated at 20, 30, and 40 kHz. The general shape of the simulated voltage waveforms agree well with the measured ones, except that the peak values are consistently lower than measurements by 30–40%. This could partly be attributed to the exclusion of the electrode voltage drop in the model. On the other hand, the peak values of the simulated currents are consistently higher than measurements by 19–52%, and the shape of the simulated current waveforms generally resemble that of the voltage indicating that the model starts behaving like a resistor prematurely at these frequencies. The measured and simulated

voltage-current characteristics are shown in Fig. 8(a) and (b) respectively, where the resistive behavior of the model is evident. Nevertheless, the model correctly predicts the trend of the characteristic varying with frequency and average power.

To test the applicability of the model at low frequency, voltage and current waveforms are measured on the 40-W lamp operated at 50 Hz from 240 V_{rms} mains using inductive ($L_b = 1$ H) ballast. The results are shown in Fig. 9(a) and (b), and the corresponding simulation results are shown in Fig. 9(c) and (d) for comparison. Except the obvious discrepancy in the peak voltage values, both sets of results do show good agreement. The hysteresis effect associated with the change of the lamp impedance or ionization state over a cycle is well predicted by the model.

Finally, the response of the model to dynamic changes in the lamp current level is investigated. This is important for testing the stability of lamp-ballast systems under abrupt transient conditions such as supply voltage fluctuation, lamp failure etc. To perform this test, the ballast frequency is stepped from 40 kHz to 20 kHz to introduce a step change in the average lamp current. The lamp's response to the step change is observed experimentally and compared to simulation in Spice. The simulation results in Fig. 10(c)–(d) show that the model copes well with the frequency step by responding quickly to the change and produces the approximately correct current values after the transition (the discrepancy in the voltage values discussed earlier remains large). Initially as the step is applied, both voltage and current increase rapidly because the electron

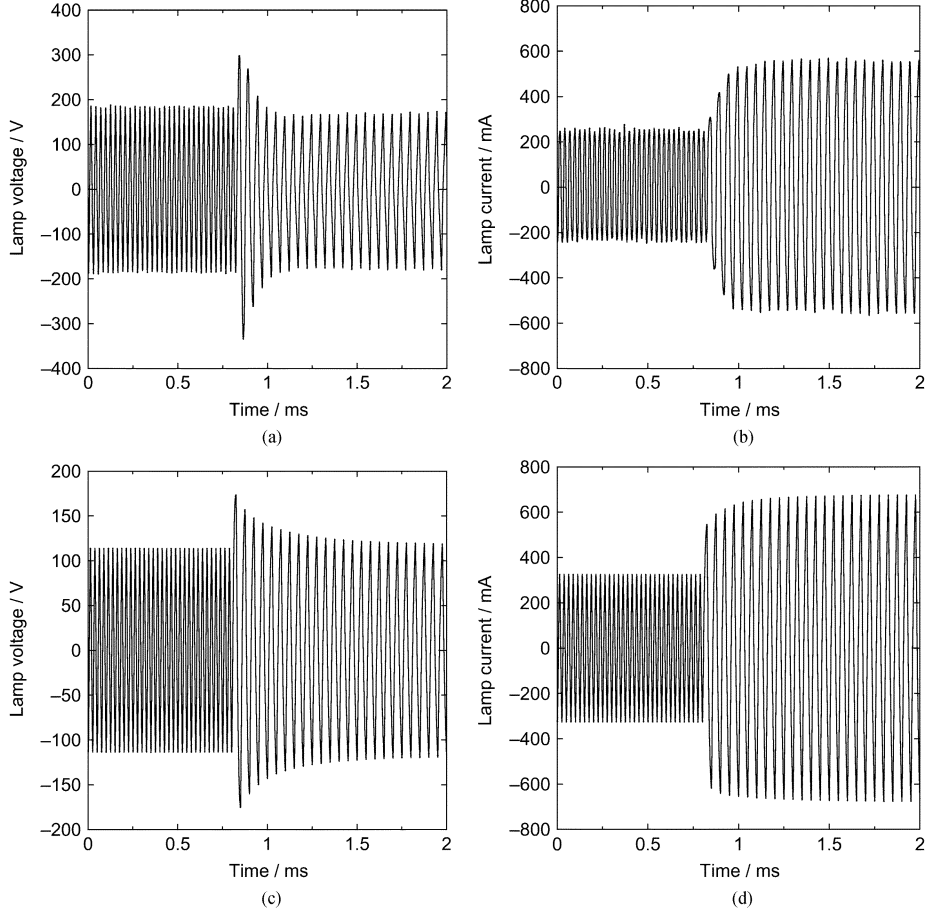


Fig. 10. Step response to a change in excitation frequency (40 to 20 kHz): (a) voltage (measured), (b) current (measured), (c) voltage (simulated), and (d) current (simulated).

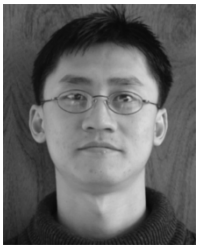
density cannot change instantaneously and the lamp behaves momentarily as an ohmic resistor. Following this the voltage decreases and the current increases gradually toward their steady state values as the lamp's conductance changes with a time lag. The predicted response time constant is about a factor of two longer than the measured value.

IV. CONCLUSION

A general conductance model of fluorescent lamp for use in both low frequency and high frequency ballast simulations is presented. The model exists in a simple exponential-integral equation derived from the time-dependent plasma ionization balance. Its implementation is compatible with circuit simulators. The model requires the user to define lamp parameters such as lamp radius, length, argon pressure and cold-spot temperature hence providing flexibility of application. Voltage and current waveforms at various frequencies and power levels have been measured and compared to simulation results, from which satisfactory agreement is obtained. The current version of the model does not predict the negative resistance behavior of discharge lamp but produces voltage values that are independent of the lamp current. This problem might be resolved by employing current-dependent functions of the gas temperature and argon pressure and further work will concentrate on obtaining expressions for these two parameters.

REFERENCES

- [1] G. Zissis, "Electrical light sources: A challenge for the future," *Eng. Sci. Education J.*, pp. 194–195, 2000.
- [2] M. Sun and B. L. Hesterman, "PSpice high-frequency dynamic fluorescent lamp model," *IEEE Trans. Power Electron.*, vol. 13, no. 2, pp. 261–272, Mar. 1998.
- [3] T. F. Wu, J. C. Hung, and T. H. Yu, "PSpice circuit model for low-pressure gaseous discharge lamps operating at high frequency," *IEEE Trans. Ind. Electron.*, vol. 44, no. 3, pp. 428–431, Jun. 1997.
- [4] S. Glozman and S. Ben-Yaakov, "Dynamic interaction analysis of HF ballasts and fluorescent lamps based on envelope simulation," *IEEE Trans. Ind. Applicat.*, vol. 37, no. 5, pp. 1531–1536, Sep./Oct. 2001.
- [5] V. Francis, *Fundamentals of Discharge Tube Circuits*. London, U.K.: Methuen & Co. Ltd., 1948.
- [6] J. F. Waymouth, *Electric Discharge Lamps*. Cambridge, MA: MIT Press, 1971.
- [7] J. O. Hirschfelder, C. F. Curtiss, and R. B. Bird, *Molecular Theory of Gases and Liquids*. New York: Wiley, 1964.
- [8] W. Schottky, "Diffusion theory of the positive column," *Phys. Zeitschrift*, vol. 25, pp. 635–640, 1924.
- [9] K. H. Loo, "A Collisional-Radiative Model of A Low-Pressure Mercury-Argon Positive Column Applicable to Steady-State and Transient Simulations," Doctoral Thesis, Dept. Electron. Elect. Eng., Univ. of Sheffield, Sheffield, U.K., 2002.
- [10] K. H. Loo, G. J. Moss, D. A. Stone, R. C. Tozer, M. Jinno, and R. Devonshire, "A dynamic collisional-radiative model of a low-pressure mercury-argon discharge lamp: A physical approach to modeling fluorescent lamps for circuit simulations," *IEEE Trans. Power Electron.*, vol. 19, no. 4, pp. 1117–1124, Jul. 2004.
- [11] J. R. Roth, *Industrial Plasma Engineering—Volume 1: Principles*. Bristol, U.K.: IOP, 1995.
- [12] C. Kenty, M. A. Easley, and B. T. Barnes, "Gas temperatures and elastic losses in low pressure mercury-argon discharges," *J. Appl. Phys.*, vol. 22, no. 8, pp. 1006–1011, 1951.

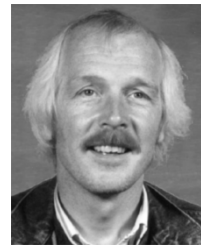


column contraction of rare gas discharges.

Dr. Loo is a member of the IEE.

Ka Hong Loo (M'99) received the B.Eng. and Ph.D. degrees in electronic engineering from the University of Sheffield, Sheffield, U.K., in 1999 and 2002, respectively. His Ph.D. research focused on the application of physical models for fluorescent lamps to ballast design, with emphasis on optimizing the discharge system running in pulse excitation mode.

He then was a Postdoctoral Researcher with Ehime University, Ehime, Japan, where he focused on the modeling study of mercury-free fluorescent lamps, including the electrode-less lamps and the positive



Richard C. Tozer (SM'98) received the B.Eng. and Ph.D. degrees from the University of Sheffield, Sheffield, U.K., in 1970 and 1975, respectively.

Following a period of postdoctoral research at the University of Sheffield in the area of CCD device applications, he became a Lecturer at the University of Essex, Colchester, U.K., where he researched active sound cancellation. In 1980, he returned as a Lecturer to Sheffield where he now teaches analogue circuit design. His research involves the application of analogue circuits to a wide range of experimental and in-

strumental problems and is currently centered around APD noise measurement and novel excitation modes for fluorescent lamps.

Dr. Tozer is a Chartered Engineer and a member of the IEE.



Dave A. Stone received the M.S. degree in electronic engineering from Sheffield University, Sheffield, U.K., in 1985 and the Ph.D. degree from Liverpool University, Liverpool, U.K., in 1989.

Since joining the Department of Electronic and Electrical Engineering, Sheffield University, in 1989, he has been interested in the industrial applications of power electronics, and is currently a Senior Lecturer.



Robin Devonshire received the B.Sc. degree in chemistry from Durham University, Durham, U.K., in 1965 and the Ph.D. degree in chemistry from Newcastle-Upon-Tyne University, Newcastle-Upon-Tyne, U.K., in 1968.

He then was a Postdoctoral Fellow in Newcastle-Upon-Tyne University from 1968 to 1969, and with Cornell University, Ithaca, NY, from 1969 to 1972. He was a Visiting Professor at King Fahd University, Dhahran, Saudi Arabia in 1991. He is now a Senior Lecturer with the Department of Chemistry, Sheffield University, Sheffield, U.K.. With the establishment of High Temperature Science Laboratories (HTSL), he is now actively involved in the research of plasma and surface diagnostics, Raman spectroscopy, high temperature chemical kinetics and thermochemistry, computational fluid dynamics (CFD), and photochemistry.